https://doi.org/10.5194/esurf-2021-53
Preprint. Discussion started: 19 July 2021

Earth Surface Dynamics Discussions
Open Access
EGU

Modeling Supraglacial Ponding and Drainage Dynamics: Responses to Glacier Surface Topography and Debris Flux Conditions

Da Huo[1] and Michael P. Bishop[1]

[1]Texas A&M University, Department of Geography, College Station, Texas, USA

Correspondence: Da Huo (dh21@tamu.edu)

Abstract. Supraglacial ponds play a significant role in the mass loss of many debris-covered glaciers in the Himalaya. Glacier surface topography and debris flux conditions are thought to govern supraglacial ponding and drainage. Existing studies, however, have not adequately investigated the relationships and feedbacks between meltwater production, debris transport, topographic evolution and ponding, because field measurements are limited in time and space, and most existing models either neglect these processes or use oversimplified assumptions. Such limitations restrict our understanding of supraglacial hydrology and introduce uncertainties in our assessments of glacier sensitivity to climate forcing. This study develops a more comprehensive numerical model to provide insights into the couplings between topographically-controlled surface ablation, meltwater drainage, ponding, and gravitational debris transport under radiative forcing. We investigate supraglacial ponding and drainage dynamics in response to different topographic and debris flux conditions through numerical simulations based on Baltoro Glacier in the Karakoram and several hypothetical scenarios. Results suggest that: 1) Supraglacial ponds make a significant contribution to the total ice loss (more than 20%) in the lower-mid ablation zone over one ablation season, which elevates the glacier's nonlinear response to radiative forcing. 2) Gravitational debris transport has a non-negligible control on the growth rate of supraglacial ponds by governing debris thickness and ablation rates on the ice-cliffs around ponds. 3) Glacier surface gradient and local topographic depressions control pond formation by affecting supraglacial water storage and drainage. Our simulations provide a possible explanation to the abundance of ponds in the mid ablation zone where slope is gentle and more local depressions are present. These findings may contribute to more accurate predictions of future glacier changes in response to climate change.

1 Introduction

Supraglacial ponds play an important role in glacier mass-balance and glacial hydrology (Fountain and Walder, 1998; Sakai et al., 2000; Wessels et al., 2002; Cuffey and Paterson, 2010; Miles et al., 2016, 2018; Huo et al., 2021a), and they are likely to grow rapidly on debris-covered glaciers (DCGs) given projections of atmospheric warming (Benn et al., 2001; Gibson et al., 2017), which will have a significant impact on regional water resources and hydro-power supply (Wessels et al., 2002; Dobreva et al., 2017; Bush et al., 2020). A typical lifespan for a supraglacial pond on Himalayan glaciers ranges from a few months to a few years, during which they can form, grow, merge and be completely drained when they intersect with englacial conduits (Benn and Lehmkuhl, 2000; Gulley and Benn, 2007). Many supraglacial water bodies are hydrologically connected

https://doi.org/10.5194/esurf-2021-53
Preprint. Discussion started: 19 July 2021


Earth Surface Dynamics Discussions
Open Access
EGU

(Watson et al., 2016; Benn et al., 2017; Miles et al., 2017), and most of them exhibit periodic filling and drainage processes (Wessels et al., 2002). Large supraglacial ponds can also be destructive, outburst floods originate from DCGs in the Himalayas have caused injuries, deaths and property damage to downstream villages (Reynolds, 2000; Richardson and Reynolds, 2000). Therefore, a better understanding of the processes and factors that govern supraglacial pond formation and evolution is critical for a more accurate assessment of regional water resources and geohazard conditions.

Supraglacial ponds and adjacent ice-cliffs are considered zones of rapid melting on DCGs (Sakai et al., 2000, 2002; Reid and Brock, 2014; Miles et al., 2016; Thompson et al., 2016; Mertes et al., 2017; Huang et al., 2018; Miles et al., 2018). A better understanding of pond dynamics can provide valuable insights into the nature of glacier sensitivity to climate change (Reynolds, 2000; Gibson et al., 2017; Benn et al., 2017; Miles et al., 2018; Huo, 2020). Field studies in the Himalaya have suggested that the degree of glacier surface lowering is related to the spatial density of supraglacial ponds in the ablation zone due to more efficient heat absorption and ablation caused by ponds (Benn et al., 2012; Miles et al., 2017). Most existing knowledge of supraglacial ponds is gained from field measurements or remote-sensing-based analysis, these field studies provide valuable insights into pond dynamics, however, they are usually limited in time and space, and do not permit a quantitative understanding of the relationship between ponding and multiple surface processes. For example, we do not know what percentage of ice-mass loss on a DCG is due to the presence of supraglacial ponds, and what are the factors and processes that control pond expansion. Supraglacial ponding is also neglected in most existing glacier models due to the complexity of characterizing the coupling between meltwater production, morphological evolution and hydrological processes. These limitations often lead to an underestimation of ice loss on DCGs. This could be, for example, one of the reasons why current models cannot explain the increasing number of supraglacial water bodies and accelerated surface lowering observed on some debris-covered Himalayan glaciers (Kääb et al., 2012; Fujita et al., 2014; Huang et al., 2018). Therefore, an integrated model that accounts for the evolution of supraglacial ponds and surface ablation dynamics is sorely needed to investigate the mass balance of DCGs and their sensitivity to climate change.

The development of supraglacial ponds on a DCG is not only governed by meltwater drainage and filling, but is also strongly controlled by topographic conditions and debris-flux. Studies have suggested that the morphological changes on a glacier surface contributes to the increasing number of supraglacial ponds (Quincey and Glasser, 2009; Benn et al., 2012), For example, the undulating surface and the gentle slope of the ablation zone on a DCG encourages the formation of ponds in depression areas (Sakai et al., 2000; Benn et al., 2001; Wessels et al., 2002; Benn et al., 2017; Miles et al., 2017), and the expansion of ponds further lowers the slope that encourages meltwater accumulation. The distribution and movement of supraglacial debris also controls pond expansion. Studies have identified significantly reduced debris thickness due to ponding (Rounce et al., 2018), and sediment flow on ice-cliffs during their retreat (Benn and Owen, 2002; Sakai et al., 2002) , which explains why the pond-facing slopes usually have a thinner debris cover that enhances melting, creating steeper slopes, and causing further retreat of ice-cliff (Sakai et al., 2002; Reid and Brock, 2014; Mertes et al., 2017). Unfortunately, the impacts of topographic condition and debris transport on supraglacial ponding dynamics have not been adequately characterized in existing models, which limits our understanding of multi-scale surface morphological evolution on DCGs.

https://doi.org/10.5194/esurf-2021-53
Preprint. Discussion started: 19 July 2021

The main objective of this study is to provide insights into the above issues by developing and evaluating a numerical model to better understand supraglacial ponding and the associated controlling factors. Specific research objectives are: 1) Develop a numerical model for DCGs that integrates meltwater production, surface drainage, ponding, topographic evolution, debris transport, and the feedback mechanisms between them; 2) Quantify the potential impact of supraglacial ponds on ice-mass loss based on a case study simulation of the Baltoro Glacier in the central Karakoram; 3) Understand how gravitational debris flux controls supraglacial ponding; and 4) Investigate surface topographic conditions that govern supraglacial pond formation using numerical simulations.

2 Methods

2.1 Data

The lower-mid ablation zone of the Baltoro Glacier is simulated to evaluate the model and to answer our research questions. The Baltoro Glacier is a notable debris-covered glacier located in the central Karakoram in Pakistan, it is one of the largest temperate glaciers in the world outside the polar regions. Baltoro Glacier is an ideal glacier for studying supraglacial ponding because quantitative estimates of surface ablation rates, debris-thickness distribution and surface morphological maps (including supraglacial ponds) over the Baltoro Glacier have been produced from field measurements and remote-sensing analysis (Mihalcea et al., 2006, 2008), and a recent study has revealed an increasing number of ponds on the Baltoro Glacier (Gibson et al., 2017).

Initial surface topography conditions and land-surface parameters were derived from a 30m digital elevation model (DEM), which was generated based on the use of stereo-correlation from ASTER (Advanced Spaceborne Thermal Emission and Reflection Radiometer) satellite imagery using SILCAST software. The initial surface temperature was acquired from the ASTER surface-kinetic temperature product derived from the same ASTER imagery (acquisition date: August 14, 2004, ID: 00308142004054614) in order to maintain temporal consistency and facilitate calibration with the field measurements acquired at that time by Mihalcea et al. (2006). The air temperature measurements in 2004 on the Baltoro Glacier (measured at 2m above the surface) have been published (Mihalcea et al., 2006), we extrapolate this data to cover the entire ablation season using the modeled mean diurnal trend of air temperature variation (Collier et al., 2013) and the monthly trend based on the NCEP-CFRS reanalysis 2-m air temperature product (Reggiani et al., 2016) in the central Karakoram region. A vertical lapse rate of $0.0065 Km^{-1}$ is used following Reid and Brock (2010) to account for the decrease in air temperature with increasing elevation.

2.2 Surface Ablation Under Radiative Forcing

Solar radiation and the thermal irradiant flux from the atmosphere are the main radiative-forcing components for melting ice (Cuffey and Paterson, 2010). We use a radiation-driven glacier ablation model because the traditional degree-day factor approach is highly site-specific and cannot adequately account for debris and topographic effects (Braithwaite and Olesen,

https://doi.org/10.5194/esurf-2021-53
Preprint. Discussion started: 19 July 2021

1990; Nicholson and Benn, 2006; Huo et al., 2020). Based on the transfer of solar radiation, the two energy fluxes received by the glacier surface are the net shortwave radiation flux (Q_s) and the net longwave radiation flux (Q_l). The total shortwave surface irradiant flux in our model consists of two components: 1) the direct solar-beam irradiance; and 2) the diffuse-skylight irradiance. They are computed following Huo et al. (2021a). In this distributed model, we classify the glacier surface into three types: debris-covered ice, bare-ice or supraglacial pond. A pixel is classified as supraglacial pond if the water depth above debris surface does not fall below 0.5m. Ablation rates are calculated differently for these three surface types based upon surface energy balance.

The energy balance at the debris/air (or the ice/air) interface can be written as (Nakawo and Young, 1981; Nicholson and Benn, 2006):

$$Q_s + Q_l + Q_h + Q_e - Q_c = 0, \tag{1}$$

where Q_h is the net sensible heat flux, Q_e is the net latent heat flux, and Q_c is the conductive heat flux into the debris or ice which governs ablation. Note that in this 2-D distributed model, heat flux terms are computed at the beginning of each iteration due to the changing topography, albedo, and surface temperature. The typographically-controlled net radiation fluxes (Q_s, Q_l) at the glacier surface and surface albedo for debris-covered area are computed following Huo et al. (2021a), Q_h and Q_e are computed following Nicholson and Benn (2006).The surface albedo of supraglacial pond as a function of water depth are estimated using the empirical equation reported by Taylor and Feltham (2004). Based on the energy balance at the ice/air interface, the melt rate for bare ice under temperate conditions can be calculated as:

$$M_i = \frac{Q_s + Q_l + Q_h + Q_e}{\rho_i L_f}, \tag{2}$$

where ρ_i is the density of ice, and L_f is the latent heat of fusion for ice.

The sub-debris ice melting is governed by the energy balance at the debris/ice interface (Nakawo and Young, 1981):

$$Q_m = Q_c^{\downarrow} - Q_c^{'}, \tag{3}$$

where Q_m is the heat flux used for sub-debris ice ablation, $Q_c^{\downarrow}$ is the conductive heat flux from the debris, and $Q_c^{'}$ is the conductive heat flux towards the ice that is not used for ablation. We assume the temperature at ice–debris interface is constant at 0°C during the ablation season after Nicholson and Benn (2006), causing $Q_c^{'}$ to be negligible (Cuffey and Paterson, 2010). Under the assumptions of constant heat storage and a linear debris-temperature gradient, Q_m during the ablation season can be estimated as (Nakawo and Young, 1981; Nicholson and Benn, 2006):

$$Q_m = \frac{k_d(T_s - T_i)}{h_d}, \tag{4}$$

https://doi.org/10.5194/esurf-2021-53
Preprint. Discussion started: 19 July 2021


Earth Surface Dynamics Discussions
Open Access
EGU

where T_i is the ice temperature, h_d is debris thickness, and k_d is the thermal conductivity of debris, which is assumed to be constant. T_s is computed for debris-covered areas at each iteration by solving equation (1) at each grid cell, and set to melting temperature for bare-ice surfaces. Then, the sub-debris melt rate M_d can be estimated as (Nakawo and Young, 1981; Nicholson and Benn, 2006):

$$M_d = \frac{Q_m}{\rho_i L_f}. \tag{5}$$

The ablation process beneath the pond surface is different from sub-debris or ice melting because pond water can store and transport energy. The energy-balance model for a closed supraglacial pond can be written as (Sakai et al., 2000):

$$Q_s + Q_l + Q_h + Q_e - \Delta Q_t - Q_{cw} = 0, \tag{6}$$

where Q_{cw} is the conductive heat flux into the ice beneath the water surface that causes ablation, and ΔQ_t is the change in heat storage of the pond (Sakai et al., 2000):

$$\Delta Q_t = \frac{c_w \rho_w \Delta T_w \Delta V_w}{\Delta t}, \tag{7}$$

where c_w is the specific heat of pond water, ρ_w is the density of pond water, and they are held as constants in our simulations. ΔT_w and ΔV_w represent the changes in water temperature and pond-volume over the time step Δt respectively. We assume a turbulent well-mixed water for the entire pond, such that the water temperature does not change with depth (Thomsen and Reeh, 1986), also note that this model neglects englacial energy transfer because we only focus on surface processes in this study.

Because ice is at melting temperature while in contact with pond water, the melt rate beneath the pond surface can be computed as (Nakawo and Young, 1981; Nicholson and Benn, 2006):

$$M_l = \frac{Q_{cw}}{\rho_i L_f}, \tag{8}$$

Collectively, the surface ablation rate M is computed differently for different surface conditions:

$$M = \begin{cases} M_i, & \text{if surface} = \text{bare-ice} \\ M_d, & \text{if surface} = \text{debris} \\ M_l, & \text{if surface} = \text{pond} \end{cases} \tag{9}$$

https://doi.org/10.5194/esurf-2021-53
Preprint. Discussion started: 19 July 2021

Surface topography evolves by a denudation rate of Δz_i after each iteration (with a time step of Δt) based upon the ablation rate and surface slope angle (θ_t):

$$\Delta z_i = M \Delta t cos\theta_t. \tag{10}$$

Note that this ablation model only accounts for the radiation-driven surface ice melt, and neglects other forms of ice-loss, such as calving around the perimeter of a supraglacial pond caused by lateral ablation, which is a process that also contributes to the expansion of ponds, because calving is governed by other processes (e.g., gravitational ice movement, ice-mass stress caused by debris load, structure of the ice-cliff and ice velocity) that are beyond the scope of this study, and cannot be characterized using the available data.

2.3 Debris Transport Around Supraglacial Ponds

Supraglacial sediment (debris) is mobile under gravity (Benn and Evans, 2014), especially during the ablation season, when the surface topography around supraglacial ponds is constantly changing (usually steepening) due to rapid melting (Sakai et al., 2002; Reid and Brock, 2014). This parameterization scheme neglects debris advection in ice-flow velocity field because we focus on the local redistribution of debris over a relatively short period of time (one ablation season), during which, the movement of debris is governed by gravity and local topographic change. From a mass flux perspective, the change of debris thickness can be estimated as:

$$\frac{dh_d}{dt} = \frac{q_{in} - q_{out}}{A_c}, \tag{11}$$

where q_{in} and q_{out} are the debris fluxes into and out of a grid cell, respectively, and A_c is the planimetric area of a grid cell. The flux out of a grid cell can be represented as:

$$q_{out} = A_s u, \tag{12}$$

where A_s is the cross-sectional surface area which the flux passes through, and u is the movement speed of a debris column. The momentum equation is used for solving u from force analysis:

$$\Delta u = \beta \frac{F \Delta t}{\rho_d V}, \tag{13}$$

where Δu represents the change in the speed of a debris column, F is the net force applied on the debris column. A tuning parameter (β) is used here to account for surface conditions that control the flux rate, and different values are evaluated in this study. The bulk density of debris (ρ_d) is assumed to be a constant, and V is the volume of the debris block. Very thin debris cover is governed by more complex dynamics: the debris is strongly affected by meltwater and ice, where cohesion and

https://doi.org/10.5194/esurf-2021-53
Preprint. Discussion started: 19 July 2021

Earth Surface Dynamics Discussions
Open Access
EGU

refreezing effects can significantly restrict debris particle movement. For simplicity, the bare-ice condition is determined as $h_d < 1$cm, following Mihalcea et al. (2008).

To estimate the net force applied on each debris column, we adopt the force analysis for unsteady gravity-driven debris flow characterized by Chen and Lee (2000), which accounts for gravity, internal friction and basal resistance for each finite moving debris column. Based on this model, the unit net force acting on a debris column, F, can be written as (Huo et al., 2021a):

$$F_x = \rho_d g[\frac{z_x}{z_x^2+z_y^2+1} - k\frac{dh_d}{dx} - \frac{1}{\sqrt{z_x^2+z_y^2+1}}\frac{u_x}{\sqrt{u_x^2+u_y^2+1}}(1-r_u)tan\varphi], \tag{14}$$

$$F_y = \rho_d g[\frac{z_y}{z_x^2+z_y^2+1} - k\frac{dh_d}{dy} - \frac{1}{\sqrt{z_x^2+z_y^2+1}}\frac{u_y}{\sqrt{u_x^2+u_y^2+1}}(1-r_u)tan\varphi], \tag{15}$$

where ρ_d is debris density, g is the gravitational acceleration constant, z_x and z_y are the first derivatives of ice-surface elevation in the E-W and N-S directions, respectively, k is the lateral Earth-pressure ratios in active state as defined by Chen and Lee (2000), u_x and u_y are debris velocity components (from previous iteration) in the E-W and N-S directions, respectively, r_u is the constant pore-pressure ratio, and φ is the dynamic internal friction angle of the debris. Figure 1 shows a sensitivity test for the β value, which controls the debris flux rate withing a reasonable range based on field observations (Huo et al., 2021b). In our numerical experiments, we vary the value of β to understand how different debris flux rates affect supraglacial ponding. Figure 2 is a diagram highlights the coupling between the local debris transport under gravity, topography and ponding, which is the main process investigated in this study.

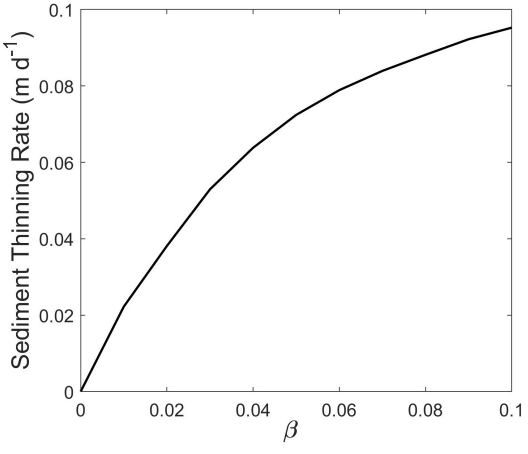

Figure 1. Sensitivity test illustrates how different β values control the rate of gravitational debris movement. Results are based on a 10-day simulation of a 20-degree inclined ice surface initially covered by 1m thick debris.

https://doi.org/10.5194/esurf-2021-53
Preprint. Discussion started: 19 July 2021

Earth Surface Dynamics Discussions
Open Access
EGU

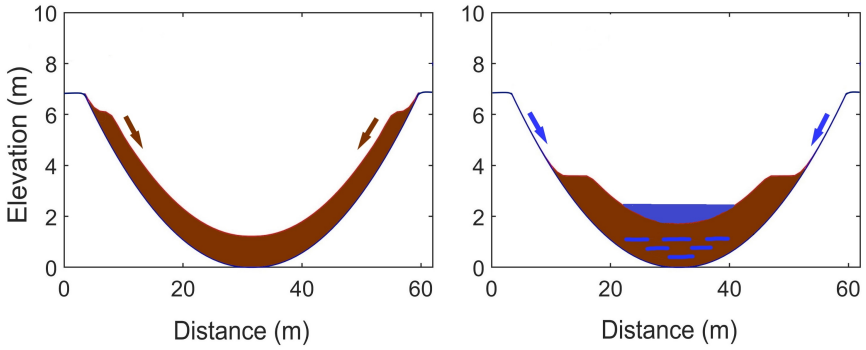

Figure 2. Diagram illustrates debris transport and ponding in a hypothetical depression. This example highlights the coupling between the local gravitational debris flux, topography and meltwater ponding.

2.4 Supraglacial Drainage and Ponding

In the ablation zone, numerous water channels form on glacier surfaces that allow efficient meltwater drainage (Cuffey and Paterson, 2010; Benn et al., 2017). A supraglacial drainage model that characterizes water-depth variation is necessary in order to simulate the formation of supraglacial ponds and to estimate meltwater runoff from the glacier surface. Based on the ablation model and the DEM of the glacier surface, we numerically simulate the supraglacial drainage and ponding conditions in the ablation season using the model presented by Lüthje et al. (2006a) and Lüthje et al. (2006b). This model is a second-order differential solution accounting for topography-controlled flow path, surface lowering due to melting, and variations in water level, and has been successfully utilized to model the evolution of supraglacial ponds and sea-ice melt ponds (Lüthje et al., 2006a,b). This model can be written as:

$$\frac{\partial h_w}{\partial t} = He(h)\left(\frac{\rho_i M}{\rho_w} - \frac{g\rho_w}{\eta}\Pi_h \nabla\cdot(h_w \nabla z_i)\right), \tag{16}$$

where h_w is water depth, t is time, $He(h)$ is a Heaviside function to prevent negative water level, ρ_w is the density of water, η is the dynamic viscosity of water, Π_h is the horizontal permeability of the debris layer that controls water-flow speed, we use a value for well-sorted gravel and sand mixture that is recommended by Bear (2013), and z_i is ice-surface elevation which is updated at each iteration based on equation (10). This model is adopted because it accounts for the resistance effect caused by a porous top layer, e.g., the barriers of porous sea ice (Lüthje et al., 2006b), which is a good analogy of modeling meltwater passing through supraglacial debris.

The timestep for the simulations is determined using an adaptive timestep approach for finite differencing implementation to ensure stability, such that the timestep for each iteration is a dynamic function of the surface gradient (∇z_i), cell size (ds) and the remaining time (t_r) for the simulation:

$$\Delta t = min(\frac{ds^2}{4max(\nabla z_i)}, t_r), \tag{17}$$

https://doi.org/10.5194/esurf-2021-53
Preprint. Discussion started: 19 July 2021

Note that this model does not account for englacial or subglacial meltwater storage and drainage, therefore, meltwater is either stored on the glacier surface or draining off of the glacier as surface runoff. Constants and default parameter values used in the simulations are listed in Table 1.

Table 1. Constants and default parameter values used in simulating ablation and pond dynamics for the Baltoro Glacier in the central Karakoram.

Constants and Default Parameter	Symbol	Value SI Units
Grid cell area	A_c	30x30 m^2
Specific heat of water	c_w	4186 $Jkg^{-1}K^{-1}$
Emissivity of air	ε_a	0.8
Emissivity of debris	ε_s	0.97
Dynamic viscosity of water	η	$1.79\times10^{-3} kgm^{-1}s^{-1}$
Acceleration of gravity	g	9.81 ms^{-2}
Debris thermal conductivity	k_d	1.00 $Wm^{-1}K^{-1}$
Latent heat of evaporation of water	L_e	$2.39\times10^{6} Jkg^{-1}$
Latent heat of fusion for ice	L_f	$3.34\times10^{5} Jkg^{-1}$
Flow-partition exponent	p	1.00
Horizontal permeability of debris	Π_h	$1\times10^{-9} m^2$
Dynamic internal friction angle of the debris	φ	0.34 rad
Lateral earth pressure ratios in active state	k	1.01
Constant pore-pressure ratio	r_u	0.5
Air density at sea-level	ρ_0	1.29 kgm^{-3}
Bulk density of debris	ρ_d	1600 kgm^{-3}
Density of ice	ρ_i	910 kgm^{-3}
Particle density of debris	ρ_p	2650 kgm^{-3}
Density of water	ρ_w	997 kgm^{-3}
Stefan-Boltzmann constant	σ	$5.67\times10^{-8} Wm^{-2}K^{-4}$
Ice temperature	T_i	273.15 K

2.5 Simulation Scenarios and Initial Conditions

Three groups of numerical experiments (Table 2) are simulated over the ablation season in 2004 to answer our research questions.

The first group of simulations (S1-S2) investigates the contribution of supraglacial ponds to the overall surface ablation and differential thinning. To quantify the ablation caused by ponds, we compare and contrast two scenarios: S1: a debris-covered glacier with supraglacial ponds, and S2: a debris-covered glacier without supraglacial ponds.

https://doi.org/10.5194/esurf-2021-53
Preprint. Discussion started: 19 July 2021

The second group of simulations (S3-S8) addresses the influences of gravitational debris flux and surface topography on pond expansion. Gravitational debris flux plays an important role in pond expansion because it controls the redistribution of debris thickness on a changing topography, and supraglacial ponds evolution could be more sensitive to the debris-flux due to the steep ice-cliffs around them. Specifically, we simulate the expansion of supraglacial ponds on different topography and with different debris-flux rates.

The third group of scenarios (S9-S11) investigates how the glacier surface gradient influences supraglacial meltwater drainage and pond formation. These simulations were designed to provide modeling evidence to support the hypothesis that a low gradient glacier surface facilitates the formation of supraglacial ponds (Reynolds, 2000). Specifically, we simulate surface drainage condition and estimate discharge for glacier surfaces with 3 different gradients at 2º, 5º, and 10º (by altering the slope of the best-fit-plane over the study glacier surface).

The initial surface topography, debris thickness distribution and meteorological measurement over the Baltoro Glacier were discussed in the data section. All scenarios start with a dry surface and we assume there is no precipitation, tributary glacier input, or englacial processes throughout the simulations, such that all supraglacial ponds are created via the accumulation of meltwater generated on the glacier surface given radiation forcing. For scenarios S3, S4 and S5, the initial topography is an inclined surface with artificial topographic variations (a hummocky surface) and a 0.5m thick debris load. For scenarios S3', S4' and S5', the initial topography is changed to an inclined surface without any undulations. For scenarios S6, S7 and S8, a subset of the actual topography on the Baltoro Glacier is used.

https://doi.org/10.5194/esurf-2021-53
Preprint. Discussion started: 19 July 2021

Earth Surface Dynamics Discussions
Open Access
EGU

Table 2. List of simulation scenarios used to provide insight into the impacts of glacier ponds on ice-mass loss and surface morphometry. The β values for low, moderate, and high debris-fluxes are 0.01, 0.05, and 0.10 respectively. HU represents the hypothetical topography with undulations, and HP represents the hypothetical inclined plane.

Simulation	ponds	Initial Surface Topography	Debris-Flux Rate
S1	Yes	Modern-day (DEM)	Moderate
S2	No	Modern-day (DEM)	Moderate
S3	Yes	HU	Low
S4	Yes	HU	Moderate
S5	Yes	HU	High
S3'	Yes	HP	Low
S4'	Yes	HP	Moderate
S5'	Yes	HP	High
S6	Yes	Modern-day (DEM)	Low
S7	Yes	Modern-day (DEM)	Moderate
S8	Yes	Modern-day (DEM)	High
S9	Yes	Gentle slope (2º)	Moderate
S10	Yes	Moderate slope (5º)	Moderate
S11	Yes	Steep slope (10º)	Moderate

3 Results

3.1 Supraglacial Ponding and Drainage

Supraglacial ponding and drainage conditions control the melt water depth distribution on the glacier surface. We simulate the supraglacial water depth variations in the ablation zone over the ablation season in 2004 (pre-existing lakes and ponds are not accounted for). Figure 3 shows the initial (Figure 3A) and final (Figure 3B) water depth distribution on the glacier surface. The final water depth distribution reveals a large number of supraglacial ponds and water channels. They are less abundant in the immediate terminus region because the debris is very thick in that area and less water can reach the top of the debris. Marginal streams are also revealed in Figure 3B, and simulation result highlights both inter-moraine and valley marginal channels, bounded by the valley walls, on both sides of the glacier. These zones represent lower surface altitudes where meltwater can accumulate and flow towards the terminus under the influence of gravity. Meltwater ponding also decreased the albedo over the glacier surface because the albedo of a supraglacial pond can rapidly drops below 0.1 with the increase of water depth (Figure 3C), as reported by previous studies (Taylor and Feltham, 2004; Lüthje et al., 2006a). Figure 3D depicts the decrease of the overall surface albedo for the study area (spatially averaged over each 30m altitude bin) from June 1st to September 28th in

https://doi.org/10.5194/esurf-2021-53
Preprint. Discussion started: 19 July 2021

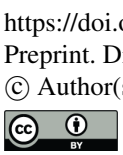

Earth Surface Dynamics Discussions
Open Access
EGU

2004, we noticed that the mid ablation zone where ponds are more abundant exhibits the most significant decrease in surface albedo over ablation season.

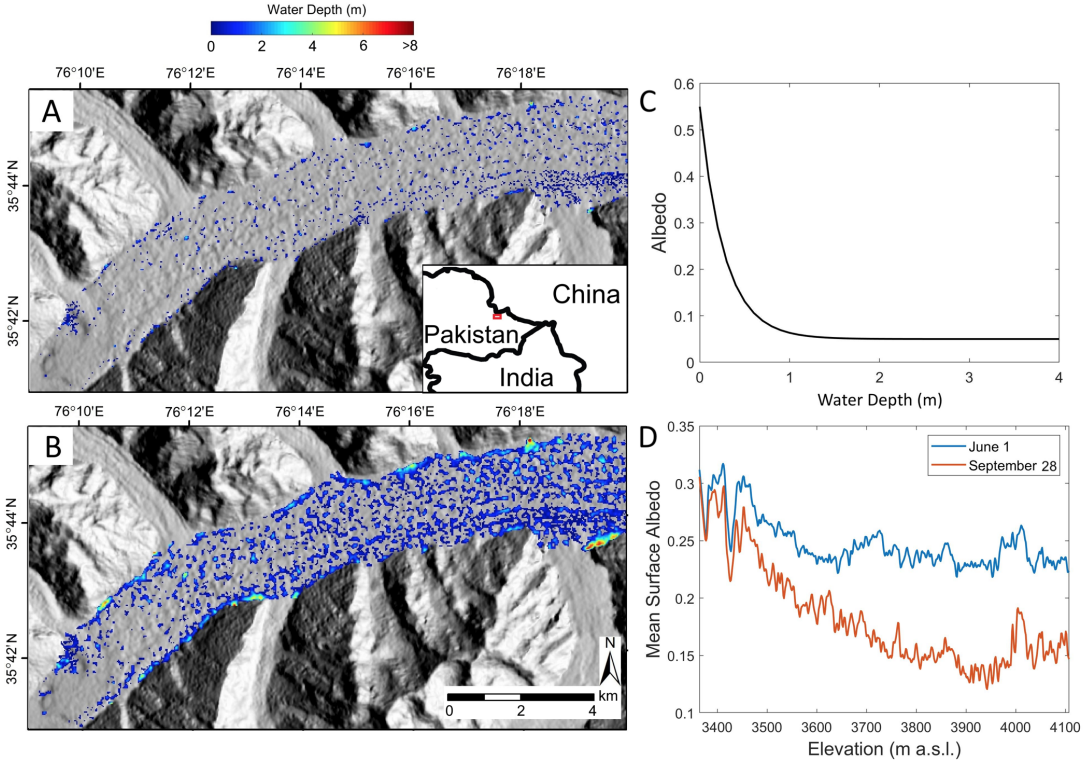

Figure 3. Simulated surface water depth in the ablation zone of the Baltoro Glacier. (A) The water depth distribution after one day of simulation (12PM on June 1st 2004). (B) The final water depth distribution (12PM on September 28th 2004). In our simulation, the surface is considered dry if the water level at that grid cell does not reach the top of debris. (C) Surface albedo of supraglacial pond as a function of water depth following Taylor and Feltham (2004) and Lüthje et al. (2006b). (D) Surface albedo over the glacier surface significantly decreased during the ablation season (from June 1st to September 28th in 2004). The altitude range with largest discrepancy corresponds to the mid ablation zone where supraglacial water bodies are most abundant.

Simulation results produce higher estimates of the total area of water bodies as compared to the published remote-sensing analysis over the same area by Gibson et al. (2017), ($1.74km^2$ versus $1.07km^2$). Many factors could contribute to this difference, both process and methodology related, for example, the quality of satellite data, and the use of thresholding can influence remote-sensing-based estimates. The dominant factor most likely is the neglection of englacial conduits in the model, as englacial conduits can rapidly reduce the volume of surface water through englacial drainage, but it is beyond the scope of this study as we only focus on surface processes. Although there is a discrepancy between the simulation and the remote-sensing results, we consider our simulations represent a meaningful first attempt to model the spatio-temporal dynamics of meltwater ponding and drainage over the ablation zone of a DCG.

https://doi.org/10.5194/esurf-2021-53
Preprint. Discussion started: 19 July 2021

3.2 Surface Ablation Due to Supraglacial Ponds

To understand how supraglacial ponds govern surface ablation, we computed surface ablation rates over the ablation season. Figure 4 compares the mean surface ablation rates and the temporal standard deviation between pond-present and no-pond scenarios (simulation S1 and S2). The mean surface ablation rates represent temporally averaged values over the ablation season (from June 1st 2004 to September 28th 2004), and the standard deviations are computed based on monthly mean ablation rates (temporal variability over the ablation season for each grid cell). The simulated sub-debris ablation rates have been validated using the field measurements, which was detailed in our previous studies (Huo et al., 2021a,b). This comparison indicates that ponds create numerous melting hotspots on the glacier surface and increased the spatial heterogeneity of surface ablation. The temporal standard deviations reveal that the ablation rates for ponds also exhibit very high temporal variability over the ablation season, which suggests that supraglacial ponds are more sensitive to the variation in radiative forcing than other areas on the glacier surface.

To better highlight ponding and its impact on the glacier, we show the increase in total surface water volume over the ablation season (Figure 4E), and temporal comparisons between the two scenarios from two perspectives: The diurnal mean ablation rate (Figure 4F), and the cumulative ice mass loss (Figure 4G). Simulation results suggest that the presence of meltwater and pond expansion dramatically accelerate the overall ice loss in the ablation zone, and the magnitude progressively increases towards the end of the ablation season because of pond expansion, although the magnitude of ablation decreases after early September, which is most likely caused by the decrease in the magnitude of irradiance. We notice that the nature of cumulative ice-mass loss is nonlinear, and we would expect that the nonlinearity can cause dramatic change over longer periods of time if the ponds remain on the surface over multi-year time frames. These results strongly suggest that the formation and evolution of supraglacial ponds represent a key indicator of a glacier's overall sensitivity to radiative forcing.

https://doi.org/10.5194/esurf-2021-53
Preprint. Discussion started: 19 July 2021

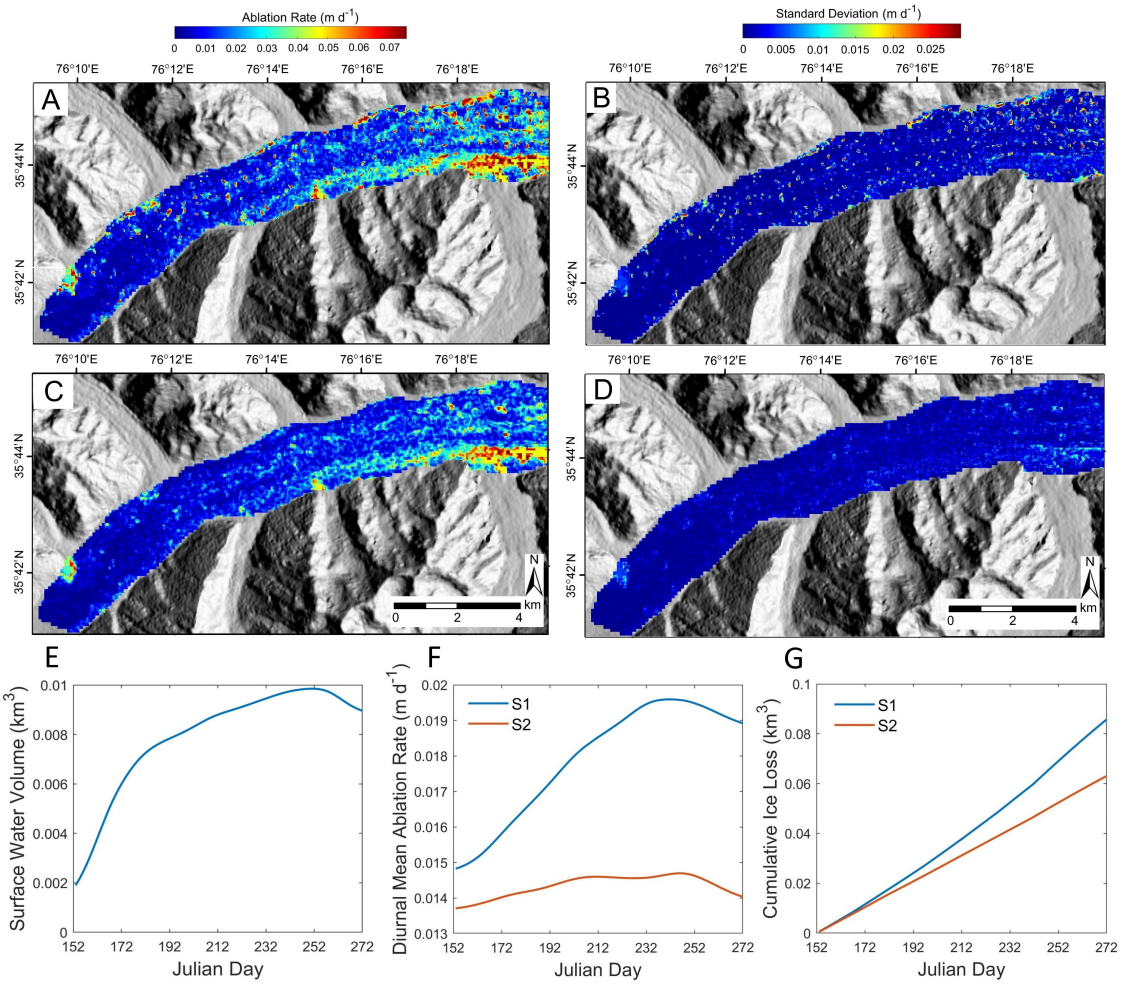

Figure 4. Comparison of surface ablation between the pond-present scenario (S1) and the no-pond scenario (S2). (A) Mean surface ablation rates for S1 (averaged over the ablation season). (B) Temporal standard deviation of surface ablation rates for S1 based on monthly-averaged results. (C) Mean surface ablation rates for S2. (D) Temporal standard deviation of surface ablation rates for S2. Plots in the third row depict temporal variations in (E) total surface water volume, (F) diurnal mean ablation rate, and (G) cumulative ice loss. Note the increased nonlinearity when supraglacial ponds are present (S1).

https://doi.org/10.5194/esurf-2021-53
Preprint. Discussion started: 19 July 2021


Earth Surface Dynamics Discussions
Open Access
EGU

Table 3. Spatial statistical comparison between simulations S1 (with ponds) and S2 (without ponds). $\bar{M}_s$ represents mean surface ablation rate, σ_{M_s} represents the standard deviation of surface ablation rate, $\bar{M}_l$ represents the mean ablation rate beneath pond surface, $A_l\%$ represents the area fraction of ponds at the end of the 120-day simulation, and $M_l\%$ represents the fraction of ponds' contribution to total surface ablation. The ablation rates are temporally averaged over the ablation season first, and then the statistics are computed over the glacier surface.

Scenario	$\bar{M}_s$ (md^{-1})	σ_{M_s} (md^{-1})	$\bar{M}_l$ (md^{-1})	$A_l\%$	$M_l\%$
S1 (with ponds)	0.0180	0.0168	0.0661	7.57%	22.78%
S2 (wihtout ponds)	0.0139	0.0126	0.0118 (debris)	0.00%	0.00%

Table 3 compares the statistics of the two simulated scenarios, which demonstrates that the presence of supraglacial ponds significantly increased the magnitude and spatial variability of surface ablation. The ponds in late September (when they reach their maximum extend) accounts for 7.57% of the surface area, but they contributed 22.78% of the total ice-mass loss over the ablation season, and the modeled ablation rates beneath the pond water are on average 5.6 times higher than the average for non-pond areas. This strongly suggests that supraglacial ponds can significantly increase ice-mass loss on a DCG, and contribute to the high-magnitude heterogeneous thinning observed on many DCGs, such as the Khumbu Glacier (Sakai et al., 2000), the Baltoro Glacier (Mihalcea et al., 2006), and the Koxkar glacier (Huang et al., 2018).

3.3 Debris Flux and Topographic Controls on Ponding

Supraglacial ponds expand during the ablation season, and the growth rate is thought to be linked with debris thickness distributions and topographic conditions around the ponds (Benn et al., 2001). To understand how debris flux and surface topography control pond expansion, we conduct simulations with three different gravitational debris flux rate and surface topography conditions (S3-S8).

Figure 5 depicts simulated ponding for simulations S3-S8, based on 1) a hypothetical topography consisting of equally-spaced periodic variations (Figure 5A); 2) an inclined surface without any topographic undulations (Figure 5B); and 3) a subset of the modern-day surface topography on the Baltoro Glacier (Figure 5C). The comparison between S3 (low flux rate scenario), S4 (moderate flux rate scenario), and S5 (high flux rate scenario) indicates a positive correlation between gravitational debris-flux rate and pond size. A higher flux rate increases pond size and water volume, and also generates higher connectivity between the ponds. This is because a faster debris-flux can dramatically decrease debris thickness on adjacent slopes by transporting debris into depression locations (e.g., ponds), which exposes large thin-debris-covered area that enhances ablation and facilitates meltwater production and pond expansion.

https://doi.org/10.5194/esurf-2021-53
Preprint. Discussion started: 19 July 2021

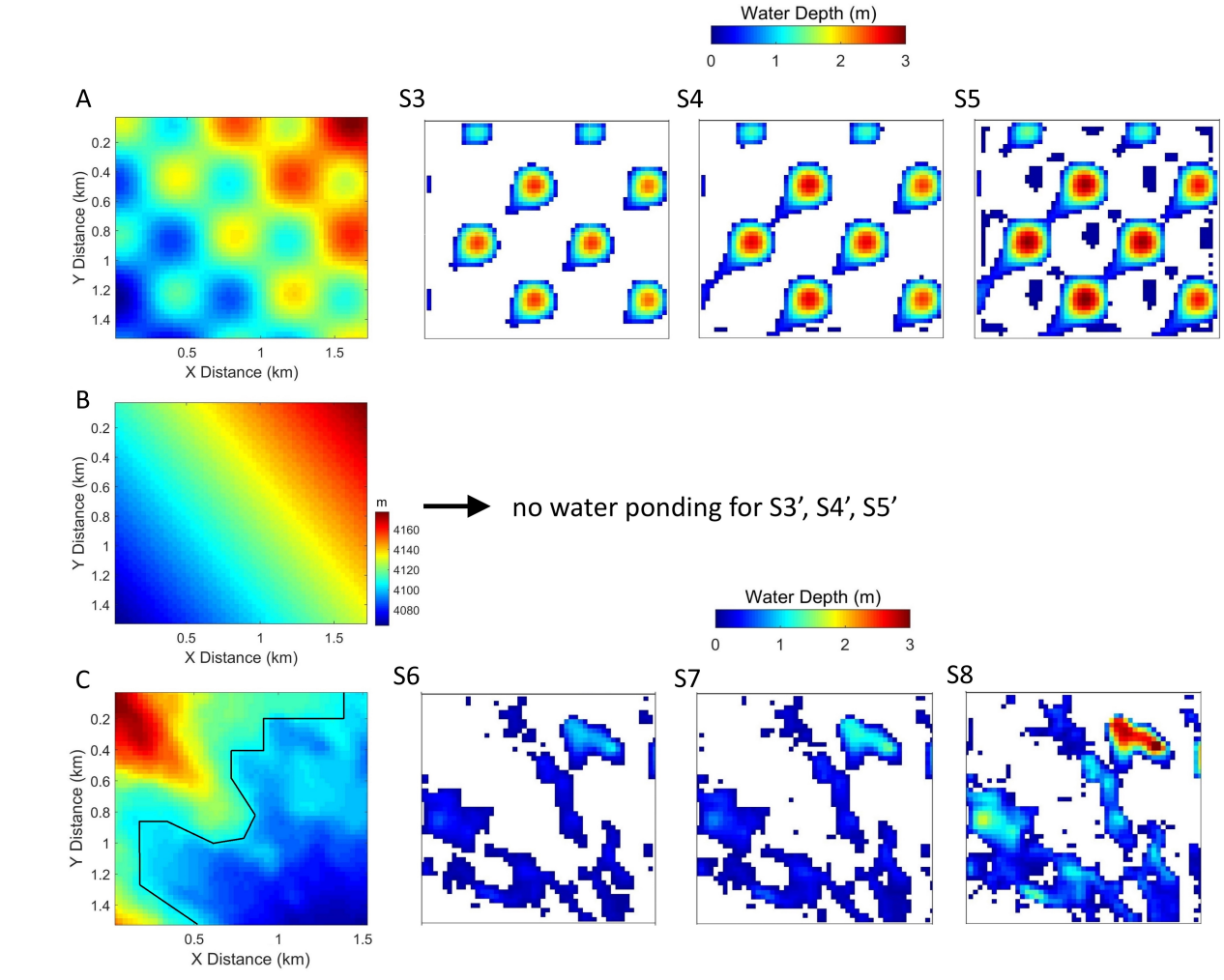

Figure 5. Simulated supraglacial ponding for three different topographic conditions. (A) A hypothetical surface with undulations, and the increase in debris flux rates (from scenarios S3 to S5) encourages meltwater ponding in depression areas. (B) A hypothetical inclined plane without any undulations does not support any water ponding. (C) A subset of the actual topography on the Baltoro Glacier, and the increase in debris flux rates (from scenarios S6 to S8) promotes meltwater ponding. These numerical experiments demonstrate that the presence of topographic depressions and the rate of debris flux have non-negligible controls on supraglacial ponding.

We then simulated pond formation on an inclined surface without any topographic undulations (S3', S4' and S5'), and simulations revealed no pond formation, as there are no topographic depressions for meltwater to accumulate. These simulations are based on unrealistic topography but they demonstrate that topographic depressions are necessary for pond formation. On the surface of an actual DCG, there are numerous depressions that would eventual accumulate water, and serve as the basis for pond growth and evolution.

https://doi.org/10.5194/esurf-2021-53
Preprint. Discussion started: 19 July 2021

To achieve a more realistic simulation, we performed numerical experiments based on modern-day surface topography, and focused on a subarea on the Baltoro Glacier (Figure 5C) where ponds are surrounded by steep slopes (early stage ice-cliffs). Similarly, we simulated the corresponding pond evolution under three different debris-flux rates (S6-S8). The bottom row in Figure 5 shows that the more intensive meltwater ponding on the glacier surface is associated with higher debris-flux rate. These results also revealed a positive correlation between the gravitational debris-flux rate and pond size, a faster sediment flux generating larger areas of thin debris on the ice-cliffs and around the pond, thereby enhancing ice melt, and producing additional meltwater that accelerates pond expansion. Given that the differential topographic lowering caused by these ponds further encourage water ponding, a positive feedback may exist between pond expansion, debris-flux, and topography that could lead to nonlinear increases in ice-mass loss on DCGs.

Note that over annual or decadal time frames, englacial drainage is a controlling mechanism on pond size, as most supraglacial ponds start to drain rapidly when they intersect englacial conduits (Benn et al., 2001). Therefore, a pond cannot infinitely expand, and our simulations only serves as a demonstration of supraglacial pond expansion before it encounters an englacial drainage channel.

Supraglacial pond evolution is also controlled by the retreat of ice-cliffs, which is a form of lateral ice-mass loss. The debris is usually thinner on the pond-facing side of the ice-cliff due to the steep slope (Figure 6A), a thin layer of debris significantly lowers the albedo when mixed with meltwater, while not providing enough insulation, which potentially leads to faster retreat if the orientation of the ice-cliff is facing the solar azimuth direction (Buri and Pellicciotti, 2018). We then compare the mean ablation rate at pond boundaries (ice-cliffs as indicated by the black line in Figure 5C) as a function of debris thickness for scenarios S6, S7 and S8 (Figures 6B, 6C, 6D). Results show the thinning of debris at pond boundaries caused by an increase in debris-flux rate, and the accelerated melt as debris gets thinner, which facilitates pond expansion. The different flux rates could be due to the different slope angles of the ice-cliff, which is a topographic control on the debris flux rate.

https://doi.org/10.5194/esurf-2021-53
Preprint. Discussion started: 19 July 2021

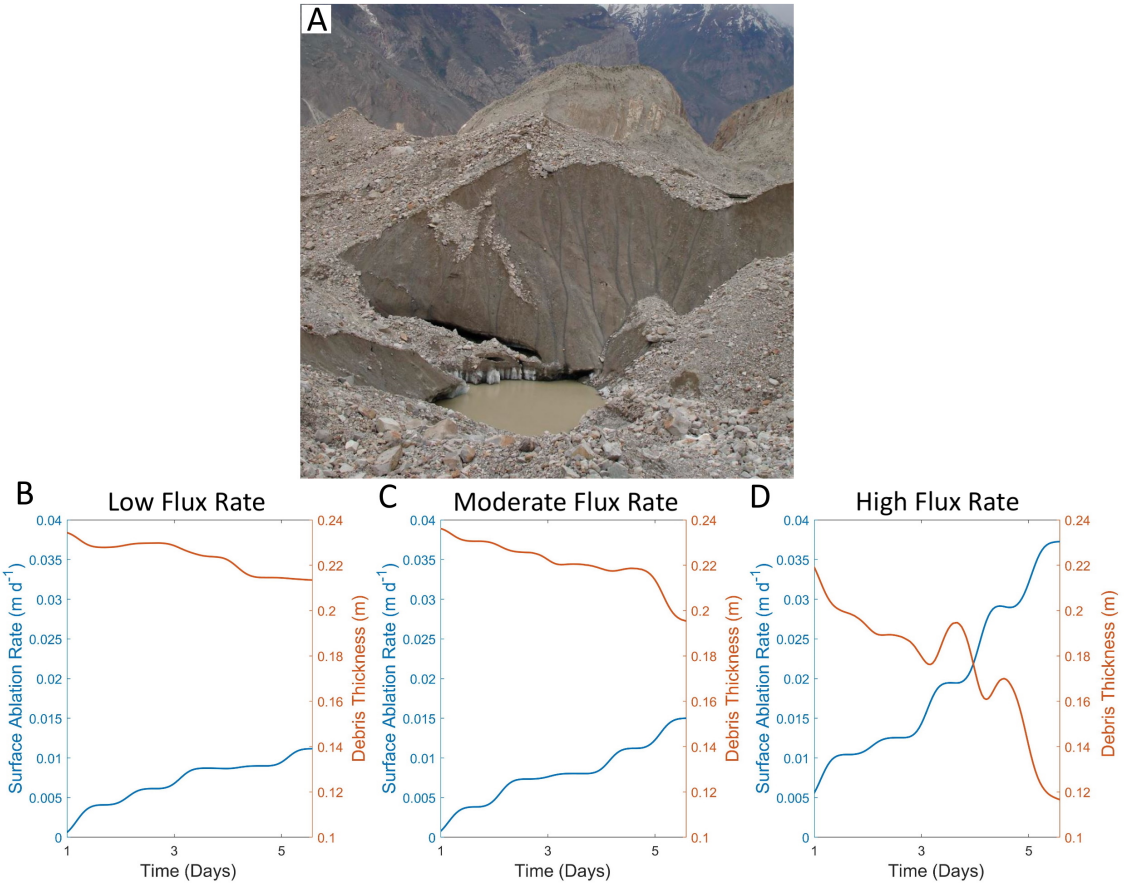

Figure 6. (A) A field photo of a debris-covered ice-cliff and a small supraglacial pond on the Baltoro Glacier during the summer of 2005 (photo credit: Andrew B.G. Bush). Note that the debris cover on the ice-cliff is thinner than adjacent areas and exhibits a relatively high moisture content (low albedo "dirty ice") due to meltwater. Simulated mean ablation rate versus debris thickness at pond boundaries are plotted for (B) A low debris flux rate scenario (S6) , (C) A moderate debris flux rate scenario (S7); and (D) A high debris flux rate scenario (S8). Note that the degree of debris thinning and ablation rate increase is regulated by the debris flux rate, which can be influenced by the topography.

3.4 Surface Gradient and Supraglacial Discharge

Field studies have suggested that the overall glacier slope gradient in the ablation zone controls the formation of supraglacial ponds, such that most ponds exist over areas exhibiting relative gentle slope (Reynolds, 2000; Sakai et al., 2002; Immerzeel et al., 2014; Reid and Brock, 2014; Thompson et al., 2016). To understand and quantify the effect of glacier surface gradient variations on supraglacial pond formation and drainage, we performed three numerical experiments on glacier surfaces with three different gradients (scenarios S9: slope angle = 2º, S10: slope angle = 5º and S11: slope angle = 10º) and investigated the variations in discharge and surface water storage (Figure 7, note that we define slope here as the overall gradient of the

https://doi.org/10.5194/esurf-2021-53
Preprint. Discussion started: 19 July 2021

entire studied ablation zone, not the local slope). The 2° (S9) scenario represents a realistic topographic condition of the study area, and scenarios S10 and S11 represent hypothetical high slope conditions. Figure 7B shows the variations in surface water volume under different slopes, and Figure 7C depicts the increase in surface discharge as the glacier surface gets steeper. Note
325 that the simulations start with an initial dry surface, so the filling process took about 25 days before the water volume and discharge stabilize. The total amount of meltwater produced from the glacier for each scenario is adjusted to be equal to the meltwater production in S9, such that surface slope is the only factor that is responsible for the difference in discharge.

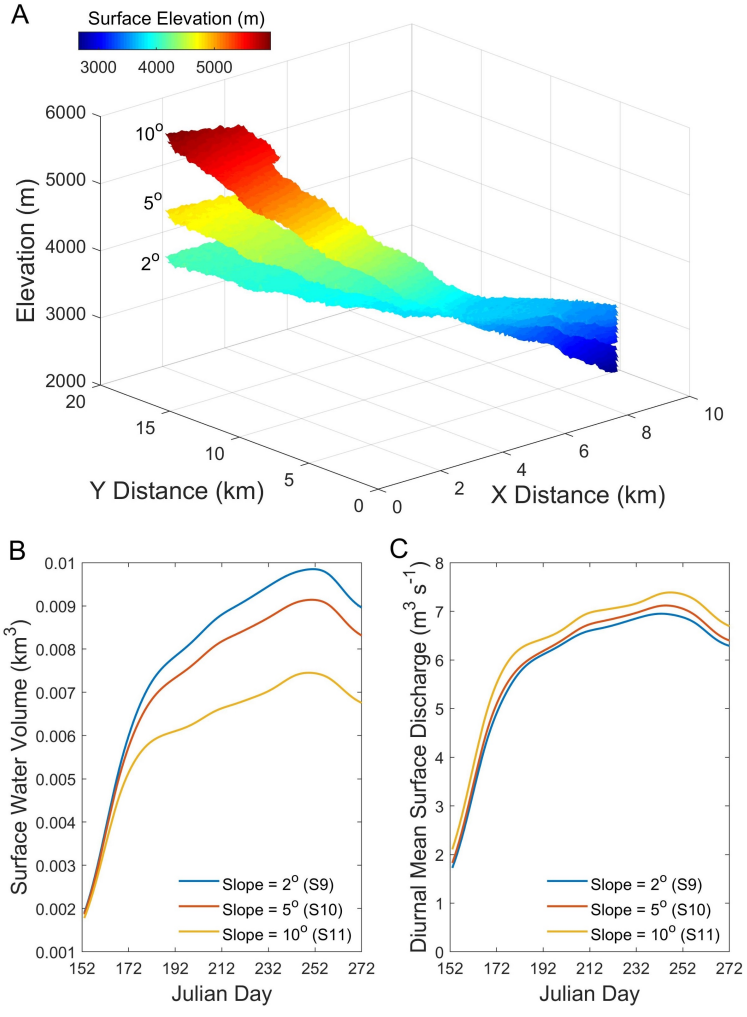

Figure 7. Glacier surface gradient control on surface water volume and supraglacial discharge as demonstrated by simulations given different slope angles. The increase in discharge and decrease in surface water volume as the glacier surface gets steeper provides a modeling evidence to the abundance of supraglacial water bodies on glaciers with a gentle altitude gradient.

https://doi.org/10.5194/esurf-2021-53
Preprint. Discussion started: 19 July 2021

The increasing discharge and decreasing water storage on a steepening glacier surface suggests that surface gradient has a significant control on supraglacial drainage efficiency. Supraglacial discharge is indicative of supraglacial pond formation because higher discharge means lower water storage on the glacier surface, which inhibits pond expansion based on our assumption of no englacial filling and drainage. The lower drainage efficiency on lower gradient indicates a higher water storage capacity on the glacier surface, which is a favored condition for pond formation. These numerical results provide a quantitative explanation for the observed abundance of supraglacial ponds in ablation zones that exhibit relatively low gradients.

4 Discussion

4.1 Supraglacial Ponds and Surface Ablation

Although supraglacial ponds and surrounding ice-cliffs only make up a very small portion of the glacier surface area, they are responsible for a significant amount of ablation that is disproportionate to their size (Table 3). Previous studies have estimated that the ablation rates around ponds can be one- or two-orders of magnitude higher than that of most debris-covered areas (Sakai et al., 2000; Benn et al., 2012; Thompson et al., 2016). Our simulation over the ablation zone of the Baltoro Glacier suggests that at least 20% of ice loss can be attributed to ponding-related ablation. This is in agreement with many field observations (e.g., Sakai et al., 2000, 2002; Reid and Brock, 2014; Anderson, 2014; Miles et al., 2016; Thompson et al., 2016; Mertes et al., 2017; Huang et al., 2018). For example, Anderson (2014) estimated that about 30% of net mass loss from the ablation zone of the Kennicott Glacier in Alaska is due to the retreat of ice-cliffs. The simulations by Miles et al. (2018) revealed that supraglacial ponds may be responsible for 1/8 of total ice loss in the Langtang valley, Nepal. Our simulated percentage based on the Baltoro Glacier fall into the range of these two studies. Supraglacial ponds can cause high-magnitude ablation and ice-mass loss for two reasons: 1) ponds efficiently absorb solar energy due to their low albedo (Sakai et al., 2000; Lüthje et al., 2006a). The energy can be effectively used for ice melt because heated pond water can easily percolate through porous debris. Sakai et al. (2000) estimated that the absorbed heat per unit area for supraglacial ponds is about 7 times higher than the average for the entire debris-covered area, and our simulations indicate that the ablation rates beneath the pond surface are on average 5-6 times higher than debris-covered ice in the ablation zone. 2) The deepening of ice surface depressions due to ponding can potentially cause faster debris transport around ponds, as more and more debris translocate and accumulate in the pond. Pond-facing ice-cliffs are usually covered by a thin layer of debris given their steep slopes (Figure 6A), which lowers the surface albedo when mixed with meltwater. Threrefore, supraglacial ponds not only enhance the vertical lowering of the glacier surface, but also encourage the lateral retreat of surrounding ice-cliffs. These processes partially explain why the glacier surface tends to be more sensitive to radiative forcing, and exhibits higher non-linearity in ice-mass loss when ponds are present (Figures 4F,4G, Table 3). We also note that supraglacial ponds significantly increased the spatio-temporal variability in surface ablation (Figures 4B,4D), given that they act as melting hotspots and vary in size and spatial density at smaller timescale than other supraglacial features. Field study has inferred a similar pattern (Huang et al., 2018), and our results provide the first modeling support to this observation.

https://doi.org/10.5194/esurf-2021-53
Preprint. Discussion started: 19 July 2021

It is important to recognize that our simulation results depict an ablation nonlinear response to radiative forcing when supraglacial ponds are accounted for, which can be characterized as an acceleration in ablation rate and total ice-mass loss. This is potentially caused by a pond's status or "stage of development", such that more rapid change is likely to occur in the later portions of the ablation season, as it reaches its yearly maximum extend and depth. As such, a nonlinear response to radiative forcing may represent the beginning of a critical transition of the glacier system that signifies a critical nonlinear response that further signifies the surface ablation-pond expansion feedback. The collective feedback mechanisms associated with supraglacial pond formation and evolution may be a sensitivity metric that indicates the rapid surface lowering of alpine debris-covered glaciers.

4.2 Topographic Control on Supraglacial Ponding and Drainage

Glacier surface topography plays an important role in meltwater ponding and drainage (Reynolds, 2000; Sakai et al., 2002). Our simulations show that glacier surface gradient controls pond formation by governing the magnitude of surface discharge (Figure 7). A higher surface gradient promotes discharge that leads to lower water storage on the glacier surface, then less supraglacial ponds could form. Therefore, the low drainage efficiency on a lower gradient surface creates the favored condition for pond formation. This phenomenon has been observed on several DCGs, where supraglacial ponds are more abundant in zones that exhibit relatively low gradients (Reynolds, 2000; Sakai et al., 2002; Immerzeel et al., 2014; Reid and Brock, 2014). Many factor contribute to the formation of supraglacial ponds, and our simulation results partially explained this phenomenon based on the gradient control on surface drainage. In addition to gradient, topographic depressions caused by differential ablation and surface water flow are also necessary for pond formation, as indicated by our simulations S3'-S5', because topographic depressions provide sinks for meltwater to accumulate. The topographic depressions are ubiquitous on DCGs given the high spatial variability in ice topography, debris thickness and ablation rate (Sakai et al., 2002; Mihalcea et al., 2008; Zhang et al., 2011; Bishop et al., 2020).

Collectively, our simulations suggest that the favorable surface conditions for supraglacial ponding on a DCG include relatively low surface gradient, presence of multi-scale topographic depressions, and heterogeneous debris thickness distribution, facilitated by the presence of meltwater and rapidly changing ice topography. Under these conditions, supraglacial ponds can form and expand rapidly if no englacial drainage occurs.

4.3 Feedback Mechanisms

Multiple processes control supraglacial ponding (Benn and Lehmkuhl, 2000; Benn et al., 2012; Huo et al., 2021c). Our model characterizes two important positive feedback mechanisms that govern pond expansion on a DCG: 1) The pond size-ablation rate feedback. As the pond grows, its surface area and surrounding ice-cliff area get larger, they absorb more solar energy which in turn accelerates ablation rate, and the retreat of these ice-cliffs leads to further expansion of the pond. 2) The ponding-surface lowering-debris flux feedback. The decrease in debris thickness is strongly related to the development of supraglacial ponds and ice cliffs (Rounce et al., 2018), and a dense spatial distribution of ponds often increases surface lowering, as they form a large number of englacial channels and the collapse of the channel roofs creates new ponds and further accelerates ablation. The

https://doi.org/10.5194/esurf-2021-53
Preprint. Discussion started: 19 July 2021

steepening of ice-cliffs at the edge of ponds encourages debris thinning, which contributes to the further expansion of ponds. This process has been described in previous studies (Reid and Brock, 2014; Miles et al., 2019), and this model provides the a numerical solution to partially simulate this positive feedback. Future work is required to include more complicated processes that also contribute to this feedback, for example, the relatively high surface temperature on ice-cliffs can produce significant emission of long-wave radiation that is part of the adjacent-terrain irradiance that also facilitates ice-cliff retreat, and ultimately further pond expansion (Sakai et al., 2002; Miles et al., 2016; Buri et al., 2016; Buri and Pellicciotti, 2018).

4.4 Assumptions and Limitations

Our simulations focus on the relationship between supraglacial ponding and glacier surface processes over one ablation season. This model does not account for precipitation forcing and ice-flow, which are known to regulate glacier mass balance, sediment fluxes and surface topography over a multi-year time scale (Cuffey and Paterson, 2010; Benn and Evans, 2014). Therefore, this model is not suitable for characterizing ablation dynamics, ponding or pond-related englacial processes over longer time periods, as other processes must be accounted for.

This model neglects adjacent-terrain irradiance, which could cause significant ablation on steep ice-cliffs (Sakai et al., 2002; Buri et al., 2016). The fluvial debris transport that could potentially decrease debris thickness and enhance ablation is also not accounted for. In addition, this model assumes no undercut on pond boundaries that causes calving and pond expansion. This model also neglects englacial filling and drainage, which are considered as an important controlling factors for many large supraglacial ponds (Benn and Lehmkuhl, 2000; Benn et al., 2001, 2017). Furthermore, this model does not account for the formation of supraglacial ponds due to the collapse of water channel roofs, which has been described in previous studies (Sakai et al., 2000). The ablation caused by warm pond water outflow is also neglected and the water temperature is assumed to be constant. Collectively, although this model accounts for more processes and feedback mechanisms than any existing models we are aware of, it may still underestimate the amount of ice-mass loss and the glacier's non-linear response to radiative forcing.

5 Conclusions

Supraglacial ponds are melt hot-spots on debris-covered glaciers. A better understanding of the ponding process provides valuable insights into the state and fate of many glaciers under a changing climate. Currently, little quantitative knowledge is known about how debris flux and surface topography control the ponding dynamics, as multiple processes and feedback mechanisms associated with pond formation and evolution have not been accounted for in existing glacier models. In this study, we investigated supraglacial ponding and drainage in response to different debris flux and topographic conditions, and quantified ponds' impact on glacier mass loss using a relatively comprehensive numerical model that characterizes surface energy balance, topographic effects, gravitational debris-flux, meltwater production, drainage and ponding. Simulation results based on the Baltoro Glacier and various hypothetical scenarios indicate that:

https://doi.org/10.5194/esurf-2021-53
Preprint. Discussion started: 19 July 2021

1. Supraglacial ponds make a significant contribution to the total surface ablation. Simulations reveal that supraglacial ponds can be responsible for more than 20% of the total ice mass loss in the lower-mid ablation zone over an ablation season on the Baltoro Glacier. The presence of ponds also elevates the spatio-temporal variability and non-linearity of surface ablation rate as they gradually reach their yearly maximum extends in the late ablation season. These nonlinear responses may indicate the beginning of critical transitions in glacier subsystem that signifies the glacier's increasing level of sensitivity to climate forcing.

2. Gravitational debris flux partially controls the expansion rate of supraglacial ponds by governing the surrounding debris thickness, such that a faster debris flux can dramatically decrease the debris thickness on adjacent ice-cliffs, which facilitates meltwater production and forms a positive feedback that further accelerates pond expansion.

3. Topographic condition also partially controls ponding, such that a glacier with low surface gradient exhibits lower surface discharge and higher surface water storage. Relatively high topographic variation also encourages pond formation. Therefore, a low surface gradient combined with a large number of topographic depressions serve as the favorable topographic condition for supraglacial ponding.

Data availability. The data used in this study is available upon request.

Author contributions. Da Huo: Conceptualization, Methodology, Data collection, Software, Model simulations, Analysis, Writing - original draft. Michael P. Bishop: Conceptualization, Methodology, Writing - review & editing.

Competing interests. The authors declare that no competing interests are present.

Acknowledgements. The authors would like to thank the GEOSAT center at Texas A&M University for providing computing resources, and NASA for making ASTER data available for researchers.

https://doi.org/10.5194/esurf-2021-53
Preprint. Discussion started: 19 July 2021

References

Anderson, L. S.: Glacier response to climate change: modeling the effects of weather and debris-cover, Geological Sciences Graduate Theses and Dissertations., 2014.

Bear, J.: Dynamics of fluids in porous media, Dover Publications, 2013.

Benn, D. and Evans, D. J.: Glaciers and glaciation, Routledge, 2014.

Benn, D., Wiseman, S., and Hands, K.: Growth and drainage of supraglacial lakes on debris-mantled Ngozumpa Glacier, Khumbu Himal, Nepal, Journal of Glaciology, 47, 626–638, https://doi.org/10.3189/172756501781831729, 2001.

Benn, D., Bolch, T., Hands, K., Gulley, J., Luckman, A., Nicholson, L., Quincey, D., Thompson, S., Toumi, R., and Wiseman, S.: Response of debris-covered glaciers in the Mount Everest region to recent warming, and implications for outburst flood hazards, Earth-Science Reviews, 114, 156–174, 2012.

Benn, D. I. and Lehmkuhl, F.: Mass balance and equilibrium-line altitudes of glaciers in high-mountain environments, Quaternary International, 65, 15–29, 2000.

Benn, D. I. and Owen, L. A.: Himalayan glacial sedimentary environments: a framework for reconstructing and dating the former extent of glaciers in high mountains, Quaternary International, 97, 3–25, 2002.

Benn, D. I., Thompson, S., Gulley, J., Mertes, J., Luckman, A., and Nicholson, L.: Structure and evolution of the drainage system of a Himalayan debris-covered glacier, and its relationship with patterns of mass loss, The Cryosphere, 2017.

Bishop, M. P., Young, B. W., Huo, D., and Chi, Z.: Spatial Analysis and Modeling in Geomorphology, in: Reference Module in Earth Systems and Environmental Sciences, Elsevier, https://doi.org/10.1016/B978-0-12-409548-9.12429-7, 2020.

Braithwaite, R. J. and Olesen, O. B.: Response of the energy balance on the margin of the Greenland ice sheet to temperature changes, Journal of glaciology, 36, 217–221, 1990.

Buri, P. and Pellicciotti, F.: Aspect controls the survival of ice cliffs on debris-covered glaciers, Proceedings of the National Academy of Sciences, 115, 4369–4374, https://doi.org/10.1073/pnas.1713892115, 2018.

Buri, P., Miles, E. S., Steiner, J. F., Immerzeel, W. W., Wagnon, P., and Pellicciotti, F.: A physically based 3-D model of ice cliff evolution over debris-covered glaciers, Journal of Geophysical Research: Earth Surface, 121, 2471–2493, 2016.

Bush, A. B. G., Bishop, M. P., Huo, D., Chi, Z., and Tiwari, U.: Issues in Climate Analysis and Modeling for Understanding Mountain Erosion Dynamics, in: Reference Module in Earth Systems and Environmental Sciences, Elsevier, https://doi.org/10.1016/B978-0-12-818234-5.00022-5, 2020.

Chen, H. and Lee, C.: Numerical simulation of debris flows, Canadian Geotechnical Journal, 37, 146–160, 2000.

Collier, E., Mölg, T., Maussion, F., Scherer, D., Mayer, C., and Bush, A. B. G.: High-resolution interactive modelling of the mountain glacier–atmosphere interface: an application over the Karakoram, The Cryosphere, 7, 779–795, https://doi.org/10.5194/tc-7-779-2013, 2013.

Cuffey, K. M. and Paterson, W. S. B.: The physics of glaciers, Academic Press, 2010.

Dobreva, I. D., Bishop, M. P., and Bush, A. B.: Climate–glacier dynamics and topographic forcing in the Karakoram Himalaya: concepts, issues and research directions, Water, 9, 405, 2017.

Fountain, A. G. and Walder, J. S.: Water flow through temperate glaciers, Reviews of Geophysics, 36, 299–328, 1998.

Fujita, K., Sakai, A., et al.: Modelling runoff from a Himalayan debris-covered glacier, Hydrol. Earth Syst. Sci, 18, 2679–2694, 2014.

https://doi.org/10.5194/esurf-2021-53
Preprint. Discussion started: 19 July 2021

Gibson, M. J., Glasser, N. F., Quincey, D. J., Mayer, C., Rowan, A. V., and Irvine-Fynn, T. D.: Temporal variations in supraglacial debris distribution on Baltoro Glacier, Karakoram between 2001 and 2012, Geomorphology, 295, 572–585, 2017.

Gulley, J. and Benn, D.: Structural control of englacial drainage systems in Himalayan debris-covered glaciers, Journal of Glaciology, 53, 399–412, 2007.

Huang, L., Li, Z., Han, H., Tian, B., and Zhou, J.: Analysis of thickness changes and the associated driving factors on a debris-covered glacier in the Tienshan Mountain, Remote Sensing of Environment, 206, 63–71, 2018.

Huo, D.: Modeling Debris-Covered Glacier Dynamics in the Karakoram Himalaya, Doctoral dissertation, 2020.

Huo, D., Bishop, M. P., Young, B. W., Chi, Z., and Haritashya, U. K.: Numerical Modeling Issues for Understanding Complex Debris-Covered Glaciers, in: Reference Module in Earth Systems and Environmental Sciences, Elsevier, https://doi.org/10.1016/B978-0-12-818234-5.00019-5, 2020.

Huo, D., Bishop, M. P., and Bush, A. B. G.: Understanding Complex Debris-Covered Glaciers: Concepts, Issues, and Research Directions, Frontiers in Earth Science, 9, 358, https://doi.org/10.3389/feart.2021.652279, 2021a.

Huo, D., Bishop, M. P., Young, B. W., and Chi, Z.: Modeling the Feedbacks Between Surface Ablation and Morphological Variations on Debris-Covered Baltoro Glacier in the Central Karakoram, (in press), 2021b.

Huo, D., Chi, Z., and Ma, A.: Modeling Surface Processes on Debris-Covered Glaciers: A Review with Reference to the High Mountain Asia, Water, 13, 101, https://doi.org/10.3390/w13010101, 2021c.

Immerzeel, W., Kraaijenbrink, P., Shea, J., Shrestha, A., Pellicciotti, F., Bierkens, M., and De Jong, S.: High-resolution monitoring of Himalayan glacier dynamics using unmanned aerial vehicles, Remote Sensing of Environment, 150, 93–103, 2014.

Kääb, A., Berthier, E., Nuth, C., Gardelle, J., and Arnaud, Y.: Contrasting patterns of early twenty-first-century glacier mass change in the Himalayas, Nature, 488, 495–498, 2012.

Lüthje, M., Feltham, D., Taylor, P., and Worster, M.: Modeling the summertime evolution of sea-ice melt ponds, Journal of Geophysical Research: Oceans, 111, 2006a.

Lüthje, M., Pedersen, L., Reeh, N., and Greuell, W.: Modelling the evolution of supraglacial lakes on the West Greenland ice-sheet margin, Journal of Glaciology, 52, 608–618, 2006b.

Mertes, J. R., Thompson, S. S., Booth, A. D., Gulley, J. D., and Benn, D. I.: A conceptual model of supra-glacial lake formation on debris-covered glaciers based on GPR facies analysis, Earth Surface Processes and Landforms, 42, 903–914, 2017.

Mihalcea, C., Mayer, C., Diolaiuti, G., Lambrecht, A., Smiraglia, C., and Tartari, G.: Ice ablation and meteorological conditions on the debris-covered area of Baltoro glacier, Karakoram, Pakistan, Annals of Glaciology, 43, 292–300, 2006.

Mihalcea, C., Mayer, C., Diolaiuti, G., D'agata, C., Smiraglia, C., Lambrecht, A., Vuillermoz, E., and Tartari, G.: Spatial distribution of debris thickness and melting from remote-sensing and meteorological data, at debris-covered Baltoro glacier, Karakoram, Pakistan, Annals of Glaciology, 48, 49–57, 2008.

Miles, E. S., Pellicciotti, F., Willis, I. C., Steiner, J. F., Buri, P., and Arnold, N. S.: Refined energy-balance modelling of a supraglacial pond, Langtang Khola, Nepal, Annals of Glaciology, 57, 29–40, 2016.

Miles, E. S., Steiner, J., Willis, I., Buri, P., Immerzeel, W. W., Chesnokova, A., and Pellicciotti, F.: Pond dynamics and supraglacial-englacial connectivity on debris-covered Lirung Glacier, Nepal, Frontiers in Earth Science, 5, 69, 2017.

Miles, E. S., Willis, I., Buri, P., Steiner, J. F., Arnold, N. S., and Pellicciotti, F.: Surface pond energy absorption across four Himalayan glaciers accounts for 1/8 of total catchment ice loss, Geophysical research letters, 45, 10–464, https://doi.org/10.1029/2018GL079678, 2018.

https://doi.org/10.5194/esurf-2021-53
Preprint. Discussion started: 19 July 2021

Miles, K. E., Hubbard, B., Quincey, D. J., Miles, E. S., Irvine-Fynn, T. D., and Rowan, A. V.: Surface and subsurface hydrology of debris-covered Khumbu Glacier, Nepal, revealed by dye tracing, Earth and Planetary Science Letters, 513, 176–186, 2019.

Nakawo, M. and Young, G. J.: Field experiments to determine the effect of a debris layer on ablation of glacier ice, Annals of Glaciology, 2, 85–91, 1981.

Nicholson, L. and Benn, D. I.: Calculating ice melt beneath a debris layer using meteorological data, Journal of Glaciology, 52, 463–470, 2006.

Quincey, D. J. and Glasser, N. F.: Morphological and ice-dynamical changes on the Tasman Glacier, New Zealand, 1990–2007, Global and Planetary Change, 68, 185–197, 2009.

Reggiani, P., Coccia, G., and Mukhopadhyay, B.: Predictive uncertainty estimation on a precipitation and temperature reanalysis ensemble for Shigar Basin, Central Karakoram, Water, 8, 263, 2016.

Reid, T. and Brock, B.: Assessing ice-cliff backwasting and its contribution to total ablation of debris-covered Miage glacier, Mont Blanc massif, Italy, Journal of Glaciology, 60, 3–13, 2014.

Reid, T. D. and Brock, B. W.: An energy-balance model for debris-covered glaciers including heat conduction through the debris layer, Journal of Glaciology, 56, 903–916, 2010.

Reynolds, J. M.: On the formation of supraglacial lakes on debris-covered glaciers, IAHS publication, pp. 153–164, 2000.

Richardson, S. D. and Reynolds, J. M.: An overview of glacial hazards in the Himalayas, Quaternary International, 65, 31–47, 2000.

Rounce, D. R., King, O., McCarthy, M., Shean, D. E., and Salerno, F.: Quantifying debris thickness of debris-covered glaciers in the Everest Region of Nepal through inversion of a subdebris melt model, Journal of Geophysical Research: Earth Surface, 123, 1094–1115, 2018.

Sakai, A., Takeuchi, N., Fujita, K., and Nakawo, M.: Role of supraglacial ponds in the ablation process of a debris-covered glacier in the Nepal Himalayas, IAHS PUBLICATION, pp. 119–132, 2000.

Sakai, A., Nakawo, M., and Fujita, K.: Distribution characteristics and energy balance of ice cliffs on debris-covered glaciers, Nepal Himalaya, Arctic, Antarctic, and Alpine Research, 34, 12–19, 2002.

Taylor, P. and Feltham, D.: A model of melt pond evolution on sea ice, Journal of Geophysical Research: Oceans, 109, 2004.

Thompson, S., Benn, D. I., Mertes, J., and Luckman, A.: Stagnation and mass loss on a Himalayan debris-covered glacier: processes, patterns and rates, Journal of Glaciology, 62, 467–485, 2016.

Thomsen, H. and Reeh, N.: Glaciological investigations at the margin of the Inland Ice north-east of Jakobshavn, West Greenland, Grønl. Geol. Unders. Rapp, 130, 102–108, 1986.

Watson, C. S., Quincey, D. J., Carrivick, J. L., and Smith, M. W.: The dynamics of supraglacial ponds in the Everest region, central Himalaya, Global and Planetary Change, 142, 14–27, 2016.

Wessels, R. L., Kargel, J. S., and Kieffer, H. H.: ASTER measurement of supraglacial lakes in the Mount Everest region of the Himalaya, Annals of Glaciology, 34, 399–408, 2002.

Zhang, Y., Fujita, K., Liu, S., Liu, Q., and Nuimura, T.: Distribution of debris thickness and its effect on ice melt at Hailuogou glacier, southeastern Tibetan Plateau, using in situ surveys and ASTER imagery, Journal of Glaciology, 57, 1147–1157, 2011.